Vietnam Journal of Science and Technology ***57*** *(3) (2019) 309-319*

doi:10.15625/2525-2518/57/2/13133

SYNTHESIS AND ANTIBACTERIAL ACTIVITY OF COMPOSITE BASED ON CHITOSAN-GRAFTED-(*N*-BUTYL ACRYLATE) AND SILVER NANOPARTICLES

La Thi Thai Ha*, Chau Ngoc Mai

Faculty of Materials Technology, Ho Chi Minh City University of Technology – VNU, 268 Ly Thuong Kiet, District 10, Ho Chi Minh City

*Email: lathaihapolyme@hcmut.edu.vn

Received: 27 September 2018; Accepted for publication: 2 January 2019

Abstract. It has been found for a long time that chitosan (CS) and silver nanoparticles (AgNPs) have outstanding antibacterial activities but there have been some drawbacks restricting a popular usage as such. Consequently, in this research, CS modified was combined with AgNPs with the purpose of expanding applications and enhancing the antibacterial activities. The colloid of CS and AgNPs (CS/Ag) was synthesized via chemical reduction while grafting copolymerization was carried out with monomer *n*-butyl acrylate (BA) and *tert*-butyl hydroperoxide (TBHP) as an initiator generating composite between CS-grafted-BA and AgNPs (CS-g-BA/Ag). The effects of synthesis parameters on the synthesizing CS-g-BA/Ag composite were studied by determining the grafting percentage (G%) and grafting efficiency (E%). The results revealed that the highest G = 80 % and E = 52 %, were obtained in the conditions as follows: the content of Ag = 0.5 %, BA/CS = 4 w/w, TBHP/CS = 7 mL/g with the concentration of TBHP aqueous solution is 20 mM, the concentration of CS is 0.85 % in acetic acid 0.6 % and assessed by Fourier Transform Infrared spectroscopy, Ultraviolet-visible spectroscopy, Differential Scanning Calorimetry, Transmission Electron Microscope, Field Emission Scanning Electron Microscope and antibacterial activity.

Keywords: antibacterial, *n*-Butyl acrylate, chitosan, grafting copolymerization, silver nanoparticles.

Classification numbers: 2.5.1, 2.5.3, 2.9.3, 2.10.2.

1. INTRODUCTION

Chitosan (CS) is a polysaccharide comprising a random distribution of ß-(1,4)-linked D-glucosamine and *N*-acetyl-D-glucosamine, which is deacetylated from chitin, one of the top plenteous natural polymers in the earth after cellulose. It is derived from the shells of crustaceans (crabs, shrimps, etc.), molluscs or insects. This polymer has a lot of features such as non-toxic, non-allergenic to human beings, biological, biodegradable and naturally biocompatible. CS has long been used as a kind of biopolymer and natural substance in numerous fields related to many utilizations in our quotidian life such as pharmaceutical and

medical industry, environmental processing, textiles, wastewater treatment, food packaging, and agriculture [1]. Having been mentioned as one of the most harmless and efficient antibacterial elements [2], this material has somewhat restricted mechanical properties, principally concerning low flexibility, brittleness as well as hydrophilicity [3].

With those disadvantages, chemical modification of CS, especially grafting with various vinyl monomers plays an integral role in manufacturing bio-materials to enhance properties without sacrificing its biodegradable nature. By this way, CS itself possesses two types of reactive sites which may possibly be modified by grafting copolymerization: C-2 amino groups in deacetylated units or the C-3 and C-6 hydroxyl groups in either acetylated or deacetylated units [3]. There are many monomers used for grafting copolymerization such as vinyl acetate [4], acrylonitrile [5], methyl methacrylate [1], PEGylated [6], etc.

Recently, in the biological areas, a lot of researchers have investigated colloid containing silver nanoparticles (AgNPs) due to its broad spectrum of excellent antibacterial activity at a low concentration, extremely safe for human beings, vegetation and all multi-celled living matter [3]. Hence, more efforts have been made to synthesize composite with the combination of AgNPs and modified CS aiming to better the weak mechanical properties and the antibacterial activity of CS.

In this paper, *n*-butyl acrylate (BA) was chosen due to its glass transition temperature (T_g) and hydrophobic attributes providing water resistance and mechanical characteristics, two vital tailored properties of CS to obtain the desired final product [3]. The synthesized copolymerization of CS was carried out with BA in the presence of AgNPs. A thorough investigation using Fourier Transform Infrared spectroscopy (FTIR), Field Emission Scanning Electron Microscope (FE-SEM), Transmission Electron Microscope (TEM), Differential Scanning Calorimetry (DSC) was made to illustrate the structure of composite CS-g-BA/Ag along with the antibacterial activity attached concurrently.

2. MATERIALS AND METHODS

2.1. Materials

CS with 70 % degree of deacetylation and M_w = 9155 from Viet Nam was filtered after being dissolved completely in acetic acid 0.6 % (AA) (China); BA (China) was purified by distillation; TBHP solution 70 % (Sigma-Aldrich) is diluted to create solution 20 mM; $AgNO_3$ (China) and $NaBH_4$ (Xilong Chemicals - China) were dissolved completely in distilled water to form solution 0.08 M and 0.03 M, respectively.

2.2. Synthesis of colloid CS/Ag

CS/Ag colloid was prepared via chemical reduction with $AgNO_3$, $NaBH_4$ as a reducing agent and CS as a stabilizer in AA solution. Firstly, CS was dissolved completely in AA to create the homogeneous mixture (with the concentrations of CS solution are 0.85 % and 1.35 %). Secondly, the amount of $AgNO_3$ aqueous solution, calculated based on the content of Ag (0.5 %; 1 % and 2 %) corresponding to the mass of CS solute, was added into 200 g CS solution under stirring 1500 rpm at room temperature in a half of hour. Finally, the freshly prepared $NaBH_4$ solution was added drop-wise into the mixture with the molar ratio of $NaBH_4/AgNO_3$ is 1:1 in 1 hour. The CS/Ag colloid was stored at room temperature for determining characteristics and following reactions.

The effect of reactants was investigated by changing CS concentration and content of silver.

2.3. Grafting copolymerization CS-g-BA/Ag

First, put 50 g of the prepared CS/Ag colloid into a three-necked flask. Second, purge nitrogen and stir the solution in 30 minutes at room temperature to remove air before the reaction begins. Keep the inert atmosphere during the reaction time. The amount of freshly prepared TBHP solution was added rapidly into the flask at 70 °C, which continued to heat up to 90 °C and kept in 30 minutes. Then, add BA drop-wise into the reactor system to carry out the reaction in 6 hours with the stirring technique. The obtained latex was dried at 90 °C with 1 atm in order to generate a film and remove remaining monomers. Finally, detach this film with 10 % NaOH solution, washed with distilled water until neutralized, then dried at 70 °C and 1 atm.

The influences of the ratio TBHP/CS, CS concentration (%CS) and content of Ag (%Ag) were determined by calculating grafting percentage and reaction efficiency.

2.4. Characterization of products

The Ultraviolet-visible (UV-Vis) spectra were obtained by UV-2450 SHIMADZU Spectrophotometer in the wavelength range of 200 to 600 nm of colloid samples. Under room temperature with dry air, FTIR spectra of the grafting samples before and after Soxhlet extraction, and original CS were conducted as KBr pressed discs on Tensor 27 Bruker IR spectrometer. Thermal analysis of the samples was performed with the DSC instrument. The specimens were heated at a heating rate of 10 °C.min^{-1} under the inert atmosphere (N_2) from -60 °C to 300 °C. The surface morphology of the product was examined by FE-SEM S-4800, Hitachi (Japan). TEM (JEOL – Japan JEM 1400) was used for the characterization of silver nanoparticles before and after grafting copolymerization. Soxhlet extraction is utilized to assess product via grafting percentage (G%) (1) and reaction efficiency (E%) (2) [2]:

$$G\% = \frac{\text{Mass of grafted monomer}}{\text{Mass of original polymer}} \times 100 = \frac{m_2 - m_{CS/Ag}}{m_{CS}} \times 100 \quad (1)$$

$$E\% = \frac{\text{Mass of grafted monomer}}{\text{Total mass of reaction monomer}} \times 100 = \frac{m_2 - m_{CS/Ag}}{m_1 - m_{CS/Ag}} \times 100 \quad (2)$$

in which, $m_{CS/Ag}$ and m_{CS} are the initial mass of CS/Ag nanocomposite and CS respectively, m_1 and m_2 are the mass of dried product before and after extraction.

The antibacterial ability of solution CS, colloid CS/Ag and CS-g-BA/Ag was tested directly by *S. aureus* ATCC 25923 and *E. coli* ATCC 25922 with the standard ISO 16649-2:2001 and ISO 6888-1:1999/ADM-1:2003. The tested environment is Baird Parker for *S. aureus* and EMB for *E. coli*. The concentration of bacteria is 10^{-4} – 10^{-2} CFU/mL.

3. RESULTS AND DISCUSSION

3.1. Mechanism of grafting polymerization CS-g-BA/Ag

Plausible grafting mechanisms are proposed in Figure 1: The initiator *tert*-butyl hydroperoxide firstly interacts with $–NH_2$ (amino groups) on the backbone of CS, generating redox pairs. At the following stage, transmission of an electron from nitrogen to hydroperoxide groups creates a nitrogen cation radical and an alkoxy radical. The nitrogen lost a proton, led to the form of an amino radical, which was feasible to initiate the graft copolymerization of BA.

The produced alkoxy radio can either initiate homopolymerization of BA in the polymeric micelles or abridge a hydrogen atom from the backbone, thereby forming a backbone radical that can initiate BA grafting copolymerization.

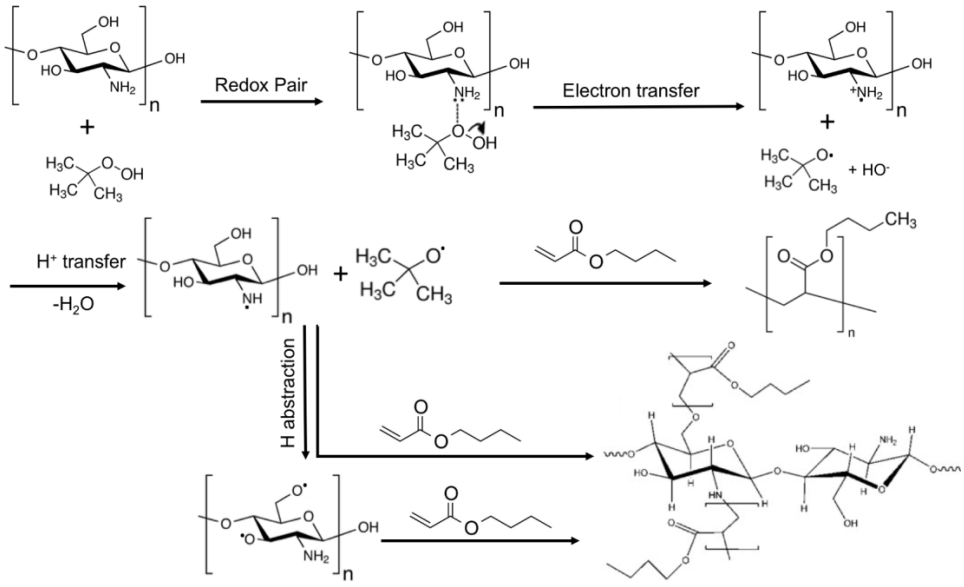

Figure 1. Proposed mechanism for grafting BA into polymers containing amino groups [7].

3.2. Effect of CS and Ag content on UV-Vis spectra

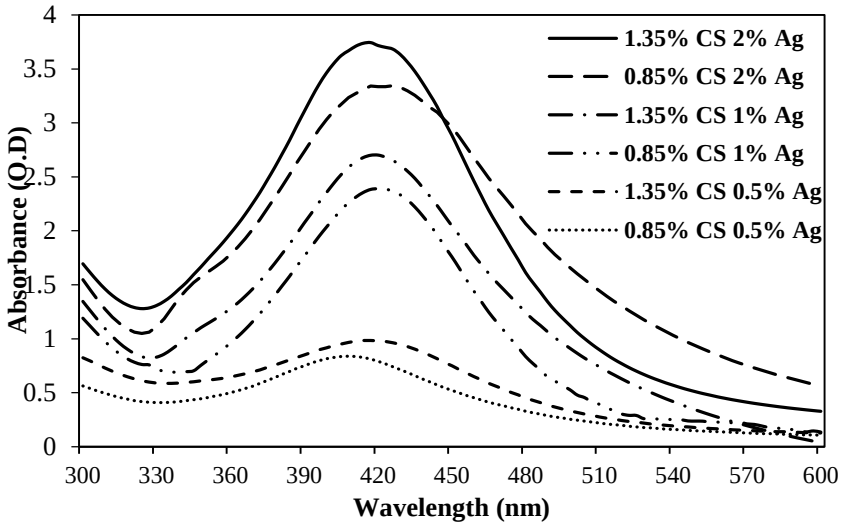

Figure 2. UV-Visible absorption spectra of colloid CS/Ag with different CS and Ag contents.

The UV-Vis spectra of CS/Ag shows clear peaks in the range 410 – 420 nm, appropriate to article of other researchers [8]. The absorption of UV-Vis spectra in Fig. 2 is affected by altering CS contents (0.85 % and 1.35 %) and content of silver (0.5 %, 1 %, and 2 %). In particular, there are the same upward trends in the intensity of the absorption peak when Ag content was fixed

and CS content increased from 0.85 % to 1.35 %. It is noticeable that the protecting agent was not utilized in the reaction system and the $NaBH_4$ was just sufficient to form silver nanoparticles. Therefore, CS here acted as a dispersing solution and a stabilizing agent to avoid agglomeration of silver nanoparticles. As a result, as the CS content increases, the growth and aggregation abilities decrease.

Regarding the rise of Ag content, unsurprisingly, the absorption peak rises dramatically when the Ag content increases from 0.5 % to 2 % in any concentration of CS. In brief, the AgNPs prepared with 1.35 % CS and 2 % Ag were formed more than other conditions (the highest intensity peak).

3.3. Effect of CS and Ag contents on grafting parameters

In Figure 3, there are similarly upward trends in G% with the increase of initiator (TBHP) and reach the highest point at 7 mL/g. Then, G% goes down in most of the situations when the amount of initiator TBHP over 7 mL/g. At the same time, downward trends in E% can be seen with the rise of the initiator from 3 to 8 mL/g ascribed to a higher amount of homopolymer formation. As I described, the more initiator is added, the more *tert*-butoxy and hydroxyl free radicals are produced that subsequently initiate the homopolymerization of BA and grafting copolymerization. If the number of free radicals is too high, radicals can be destroyed entailing the decrease of radicals in solution. It does generally affect G% and E%.

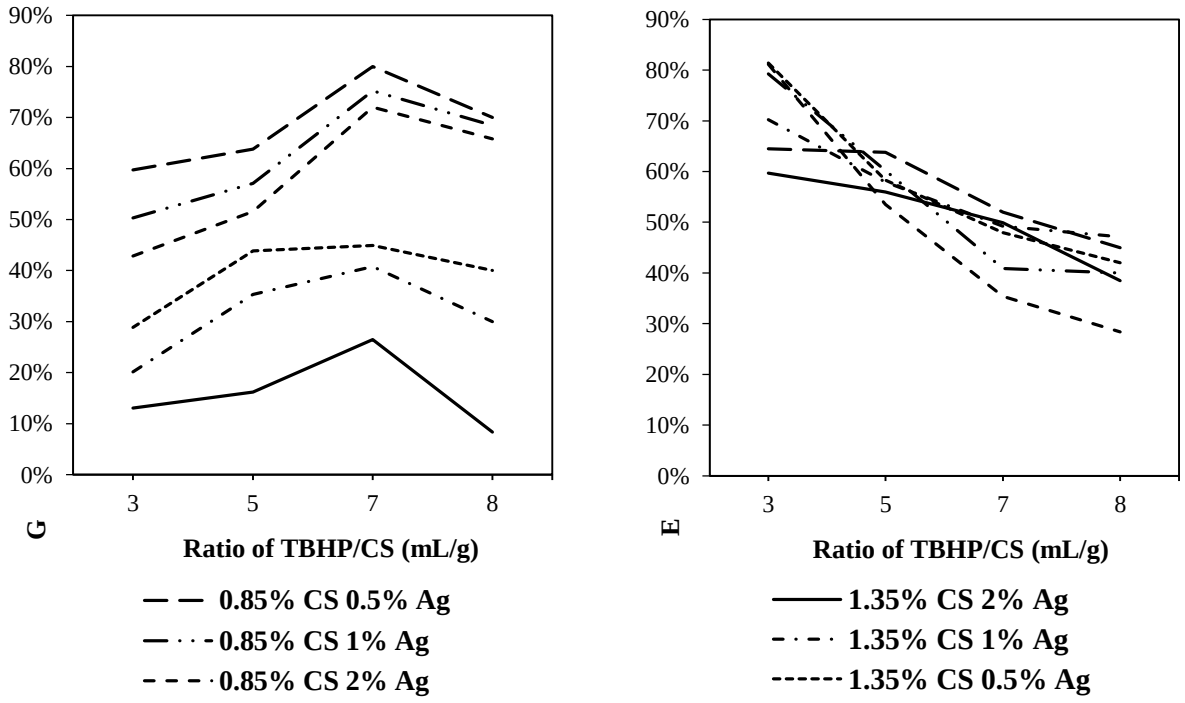

Figure 3. Effect of CS and Ag contents on G% and E% with the increase of TBHP/CS.

On the other hand, a comparison of the dominant points from Fig. 3 indicates that at the same Ag content (2 %, 1 % or 0.5 %), the higher the CS content is, the lower the G% obtained.

This means that at high CS concentration, these molecules were shielded and interacted with each other. While at the low CS content, polymer chains can stretch freely, facilitating the creation of backbone macroradicals initiating the grafting copolymerization.

Meanwhile, it is important that the increase of Ag content restricts the growth of both G% and E% and affects the polymer structure. Specifically, the highest G% was obtained roughly 80 % with 0.5 % Ag, followed by approximately 70 % with 2 % Ag corresponding to the relatively equal E (52 %). Similar to Na^+ ions, the amount of AgNPs is considered as Ag ions because the amount of $NaBH_4$ and $AgNO_3$ was used in equal proportions. Those could interact with $–NH_2$ and –OH on the CS backbones, thereby entailing CS molecules to stretch from shrinking state owing to cationic properties of CS. The active groups $–NH_2$ and –OH might be shielded and covered; thus, less $–NH_2$ and –OH are able to react with free radicals to initiate for grafting copolymerization, which is correspondingly the decline of G and E [1].

In this study, the highest G = 80 % and E = 52 % were achieved with the conditions as follows: CS concentration 0.85 %, content of Ag 0.5 % and the ratio of TBHP/CS 7 mL/g. This best sample was evaluated to demonstrate grafting copolymerization, observe morphology and examine antibacterial activity.

3.4. Assessment of the sample having the highest G% and E%

3.4.1. FTIR spectra

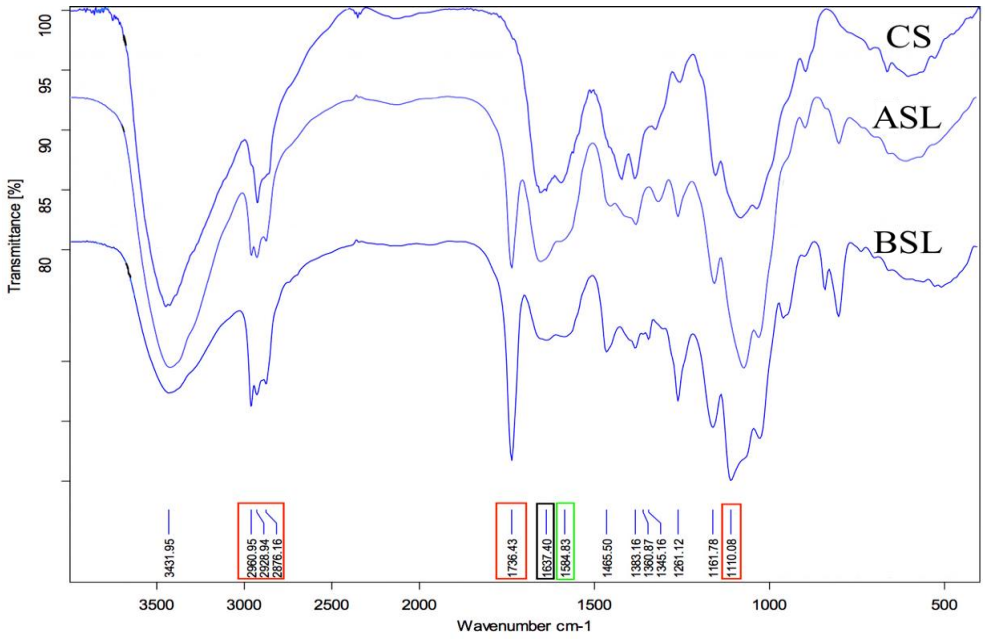

Figure 4. FTIR spectra of chitosan (CS), product CS-g-BA/Ag before and after Soxhlet extraction (BSL and ASL, respectively).

As seen from the FTIR spectra of CS (Fig. 4), most of the visual peaks are associated with carbohydrate structure. The wide and strong absorption peak at 3431 cm^{-1} (OH and NH stretching), peak at 2960 – 2876 cm^{-1} (CH stretching), 1637 cm^{-1} (NH bending amide I of acetylated units in chitin), 1584 cm^{-1} (NH bending amine I) and the area around 1066 - 1100 cm^{-1} is common in spectra due to CS backbone.

Comparative analysis of the spectra of CS and product CS-g-BA/Ag before Soxhlet extraction (BSL), it shows the presence of a peak at 1736 cm^{-1}, corresponding to C=O stretch in the product. It also has the increase of C-O-C stretching peak at 1110 cm^{-1}, compared to the unchanged peak at 1637 cm^{-1} (amide I of chitin). Those represent the exist of ester bonds of BA in both homopolymer and copolymer. Concurrently, CS-g-BA/Ag after Soxhlet extraction (ASL) displays the decrease in the intensity of C=O stretch and C-O-C stretch (1736 and 1110 cm^{-1}). This proves homopolymer is eliminated from the mixture. Besides, SSL, compared with CS, can be found that the specific peak still exists at 1736 cm^{-1} (COO of BA) and the fall of the intensity at 1584 cm^{-1} (amine I). It demonstrates the success of grafting BA into CS molecules.

3.4.2. DSC

The DSC curve from Fig. 5 reveals the thermal analysis of CS-g-BA/Ag having the highest G% and E% after extracting homopolymer by Soxhlet. The first jump at about -30 °C is predicted that is the T_g of this copolymer. We knew that T_g of PBA is -54 °C [9] and the higher G% is, the closer to -54 °C T_g of that copolymer is. This indicates that the T_g is related to BA chains on the side of the CS backbones, while T_g of original CS cannot be determined on account of its brittleness. At the temperature 46 °C and 174 °C, those distinct degradable peaks are attributed to the evaporation of the used solvent (AA) in the dissolving stage and the dehydration of CS due to the fact that CS thermogram indicates the usual polysaccharide behavior [10]. In terms of the final exothermic peak at approximately 250 – 300 °C, it corresponds to the thermal decomposition for amine residues on the backbone [11].

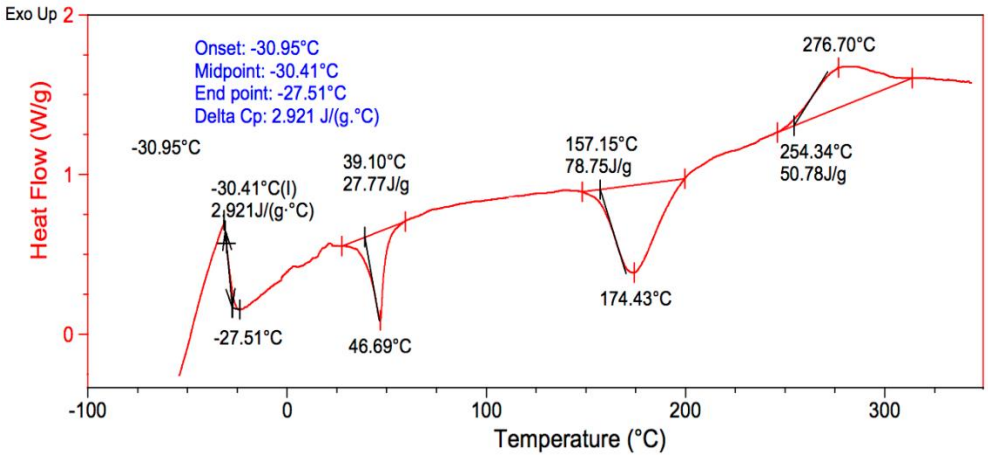

Figure 5. DSC curve of the CS-g-BA/Ag copolymer after Soxhlet extraction.

3.4.3. TEM and SEM

TEM micrographs of colloid CS/Ag in Fig. 6a illustrate the sphere shape of AgNPs in solution with the uniform particle size (approximately 5 – 6 nm). The results of latex CS-g-BA/Ag (Fig. 6b) manifests the sphere AgNPs, which remains unchanged and stable. This means that AgNPs are unaffected during the grafting period. Besides, we can see the core-shell formation of product CS-g-BA/Ag (Fig. 6c) via the mechanism related to Fig. 1: TBHP initiates grafting copolymerization in order to generate macro-radicals, and initiates homopolymerization of BA simultaneously. These amphiphilic CS-g-BA macro-radicals are self-assembly to create

macromolecular micelles including hydrophobic BA surrounded by hydrophilic CS. This phenomenon facilitates homopolymer BA in the interior, resulting in the particles with core-shell structure [12] and the relatively uniform particle size (about 200 nm).

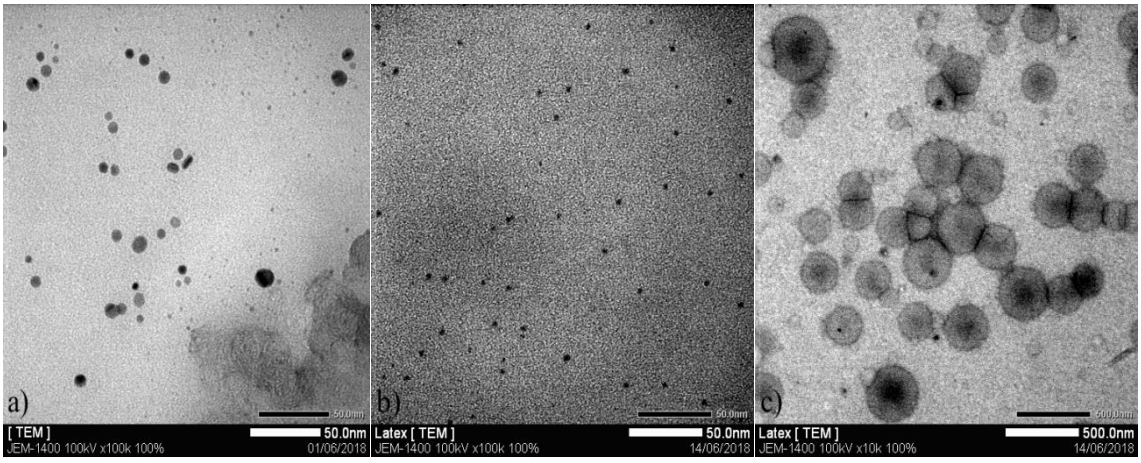

Figure 6. TEM micrographs of colloid CS/Ag (a) and latex CS-g-BA/Ag (b and c).

The FE-SEM micrographs (Fig. 7) showed the difference between the surface of dried colloid and dried latex. As observed, the formed coating of colloid has a smooth surface prior to grafting copolymerization. It is also found that the rough exterior of latex with the sphere particles, which is nearly five times as big as that of the particles in latex before drying. This can be elucidated that the solvent evaporates completely in the dried process enabling the particles to compress and combine with one another. Otherwise, other particles are deformed because the self-assembly process cannot take place as in the solution.

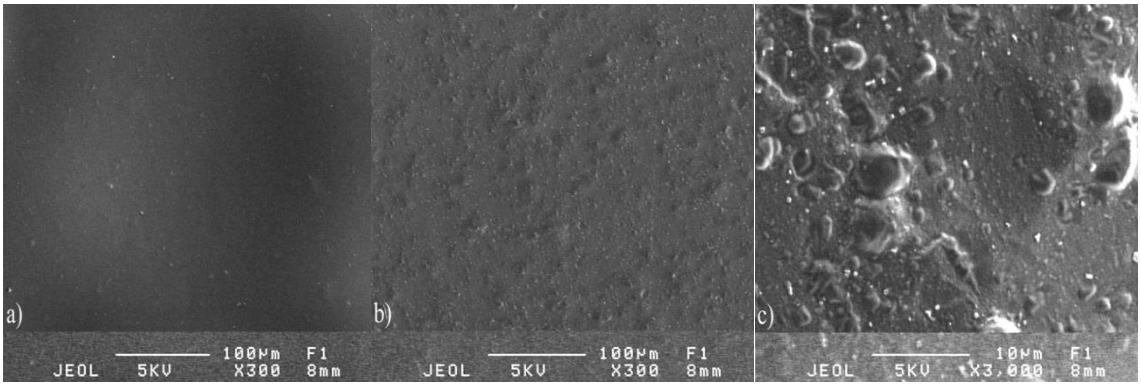

Figure 7. FESEM micrographs of the colloid CS/Ag (a) and the latex CS-g-BA/Ag after completely dried (b and c).

3.5. Antibacterial activities

Figure 9 illustrates the antibacterial rate of original CS compared to colloid CS/Ag and latex CS-g-BA/Ag by *S. aureus* and *E. coli* based on the Colony-count technique in the Petri dishes (Fig. 8). CS itself is well-known for strong antibacterial properties in both types of grams,

and Fig. 9 shows the antibacterial rate of CS is not really different (approximately 97 %) with *E. coli* and *S. aureus*. Since AgNPs outstrip original CS in terms of antimicrobial abilities, the presence of Ag could significantly enhance the antibacterial activity of CS. To specify, the antibacterial rate of CS to *E. coli* is 97 % while that of CS/Ag is over 99 % efficiency, and the rate of CS/Ag to *S. aureus* is roughly 98 %. At the same time, the antibacterial percentage of latex CS-g-BA/Ag does not decline substantially compared to CS/Ag, demonstrating that the grafted BA backbones trivially influence the antibacterial ability of the CS/Ag colloid.

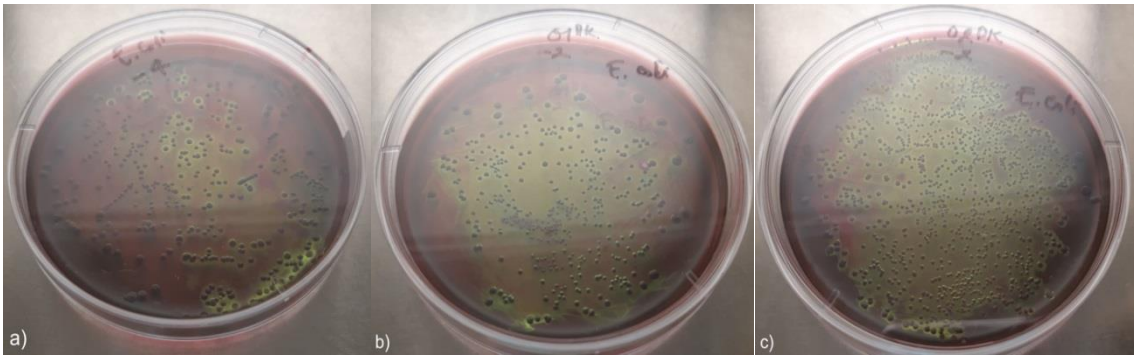

Figure 8. Pictures of the petri dishes with: a) Standard sample *E. coli*; b) Latex; c) CS.

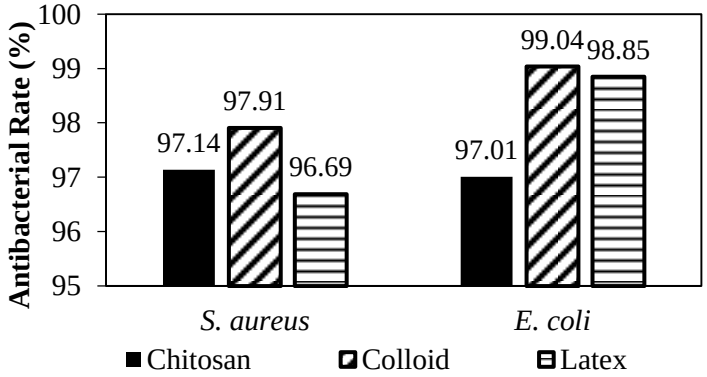

Figure 9. The antibacterial rate of CS, colloid CS/Ag and latex CS-g-BA/Ag.

In the past, many researchers have investigated the antibacterial mechanism of AgNPs as well as original CS on microorganisms that have been recorded [13-16]. In the present, the combination of AgNPs and modification based on natural materials as CS attracts interest from many scientists [9, 10, 17]. This is due to the electrostatic interaction between CS and negatively charged bacteria cell, the CS/Ag and CS-g-BA/Ag can attack the bacterial cell wall and perform a much more efficient antimicrobial ability compared to original CS, by reason of the synergistic effect of the silver nanoparticles in conjunction with CS in the composites. Besides, Jing *et al.* published the synthesized process of nanocomposite CS-grafted-(methyl methacrylate)/Ag, using CAN as an initiator [1]. His paper revealed that the antimicrobial rates of CS/Ag against *E. coli* and *S. aureus* are approximately 99 % and 98 %, relatively equal to these results while the antibacterial percentages of CS-g-MMA/Ag are 95 % and 94 %, lower than CS-g-BA/Ag in this research. Even if the content of silver nanoparticles they used is 0.72 % (higher than 0.22 % compared to this article), the antimicrobial activities with grafting MMA onto CS backbones are fewer than using BA. It can be interpreted due to the fact that G% of CS-g-BA is 80 %, greater

than CS-g-MMA (43.7 %), the number of BA engaging in the grafting copolymerization is much more than Jing's experiments, thereby leading to the predominance of antibacterial abilities.

4. CONCLUSIONS

In this article, the CS/Ag colloid and CS-g-BA/Ag composites were successfully synthesized through chemical reduction and grafting copolymerization, and these processes were confirmed by UV-Vis, FTIR spectroscopy and numerous micrographs as well. From the obtained results, it can be concluded that: There is a slight influence on the antibacterial activity caused by grafting copolymerization but CS has been improved some drawbacks with regard to less brittleness (via the appearance of T_g). The high grafting efficiency percentage is obtained at 7 mL/g TBHP/CS (G = 80 % and E = 52 %). However, both G% and E% decline dramatically if the amount of initiator is in excess. The higher content of silver is, the more significant the decrease of G% and E% is. From this, 0.5% Ag is the ideal proportion to obtain the highest grafting parameters as well as greatly improve the antibacterial rate for grafting products (roughly 97 – 99 % for both positive as *S. aureus* and negative bacteria as *E. coli*), simultaneously. CS molecules could act as a stabilizing agent to prevent the growth and aggregation of AgNPs. The CS concentration 0.85 % is better to facilitate the formation of backbone macroradicals initiating the grafting copolymerization that rises G% and E%.

REFERENCES

1. Jing A., Xiaoyan Y., Qingzhi L., Desong W. – Preparation of chitosan-graft-(methyl methacrylate)/Ag nanocomposite with antimicrobial activity, Polym. Int. **59** (1) (2010) 62-70.
2. Provder T., Baghdachi J. - Core-Shell Particles Containing Poly(n-Butyl Acrylate) Cores and Chitosan Shells as a Novel Durable Antibacterial Finish, Smart Coatings, American Chemical Society: Washington DC, 2007.
3. Anbinder P., Macchi C., Analvy J., Somoza A. - Chitosan-graft-poly(n-Butyl Acrylate) copolymer: Synthesis and characterization of a natural/synthetic hybrid material, Carbohydr. Polym. **145** (2016) 86-94.
4. Trong-Ming D., Chia-Fong K., Wen-Yen C. - Preparation of Chitosan-graft-poly(vinyl acetate) Copolymers and Their Adsorption of Copper Ion, Polym. J. **34** (6) **(**2002) 418-425.
5. Hebeish A. A., Ramandan M. A., Montaser A. S., Farag A. M. - Preparation, Characterization and antibacterial activity of chitosan-g-poly acrylonitrile/silver nanocomposite, Int. J. Biol. Macromol. **68** (2014) 178-184.
6. Quanqing L., Haiqi G., Lihua P., Gongyan L., Zongcai Z. - Synthesis of PEGylated chitosan copolymers as efficiently antimicrobial coatings for leather, J. Appl. Polym. Sci. **133** (22) (2016) 43465.
7. Pei L., Junmin Z., Panya S., Frank W. H. – New Route to Amphiphilic Core-Shell Polymer Nanosphere: Graft Copolymerization of Methyl Methacrylate from Water-Soluble Polymer Chains Containing Amino Groups, Langmuir **18** (22) (2002) 8641-8646.
8. Solmaz A., Esra D.A., Muzaffer Y., Oray E. – The Effect of Ag content of the Chitosan-Silver Nanoparticle Composite Material on the Structure and Antibacterial Activity, Adv. Mater. Sci. Eng. **2013** (2013) 1.

9. Jakubowski W., Juhari A., Best A., Matyjaszewski K. - Comparison of thermomechanical properties of statistical: gradient and block copolymers of isobornyl acrylate and n-butyl acrylate with various acrylate homopolymers, Polym. J. **49** (6) (2008) 1567-1578.
10. Roberto R. C., Maria D. V. O. – Characterization and Dissolution Study of Chitosan Freeze- Dried Systems for Drug Controlled Release, Molecules **14** (11) (2009) 4370-4386.
11. Guinesi L. S., Cavalheiro E. T. G. - The use of DSC curves to determine the acetylation degree of chitin/chitosan samples, Thermochim. Acta **444** (2) (2006) 128-133.
12. Jun-Won K., Ji Y. L., Ki S. H., In P., Jung H. K., Jun-Young L. - Synthesis and Characterization of Poly(Methyl Methacrylate)/Polyethylenimine Grafting Core-Shell Nanoparticles for CO_2 Adsorption Using Soap-Free Emulsion Copolymerization, Advances in Materials Physics and Chemistry **6** (7) (2016) 220-229.
13. Franci G., Falanga A., Galdiero S., Palomba L., Rai M., Morelli G., Galdiero M. - Silver Nanoparticles as Potential Antibacterial Agents, Molecules **20** (5) (2015) 8856-8874.
14. Guzman M., Dille J., Godet S. - Synthesis and antibacterial activity of silver nanoparticles against gram-positive and gram-negative bacteria, Nanomed-Nanotechnol **8** (1) (2012) 37-45.
15. Sung K. J., Eunye K., Nam Y. K., Jong-Ho K., Jin S. J., Jang L. H., Hyun K. S., Kyung P. Y., Ho P. Y., Cheol-Yong H., Yong-Kwon K., Yoon-Sik L., Hong J. D., Myung-Haing C. - Antimicrobial effects of silver nanoparticles, Nanomed-Nanotechnol **3** (1) 2007) 95-101.
16. Arno V., Stein M., Christian V. S. - Recent developments in antibacterial and antifungal chitosan and its derivatives, Carbohydr. Polym. **164** (2017) 268-283.
17. Metzler M., Chylinska M., Kaczmarek H. - Preparation and characteristics of nanosilver composite based on chitosan-graft-acrylic acid copolymer, J. Polym. Res. **22** (8) (2015) 1-10.